Vector-Controlled Induction Motor Drive with a Self-Commissioning Scheme

Ashwin M. Khambadkone and Joachim Holtz, *Senior Member, IEEE*

Abstract—**Different vector-controlled structures are discussed and their suitability for an economical and reliable industrial drive system is explored. From this, the design of a compact control hardware is derived, comprised of an 80196 microcontroller and an ASIC for the generation of the pulsewidth modulation (PWM) signals. The drive system can be configured from a host computer or a hand-held servicing unit through a serial data link. Monitoring and diagnostic functions are included. A self-commissioning scheme permits the setting of the parameters for optimum dynamic performance of the induction motor. Various oscillograms demonstrate the behavior of the vector controller operating a 25-kVA PWM inverter.**

I. Introduction

PULSE WIDTH modulation (PWM) inverter-fed induction motor drives are increasingly used for the operation of all kinds of industrial production and automation processes. For applications requiring high dynamic performance, the vector control principle is generally employed.

Since the first proposal [1], the structure of the induction motor vector control system has been more or less standardized to a few proven schemes [2]–[4]. The variations consist in different methods of identifying the field angle, which may be based on on-line acquired data of 1) stator voltage and stator current or 2) stator current and mechanical speed. Each model has its own advantages and disadvantages.

The design of the current controllers addresses another variety of options. The controllers can be linear or nonlinear controllers. The stator current vector and its reference value may be represented either in the stator coordinate system or in a field-oriented reference fame. The differences in performance relate to parameter sensitivity and the behavior around zero speed.

This paper discusses the available vector control structures and probes their suitability for an economic and reliable vector control scheme suitable for large-scale industrial production. Keeping in mind the falling costs of microelectronic devices, the emphasis is on full digital solutions to be implemented with the available state-of-the-art very large scale integration (VLSI) hardware.

II. The Machine Model

The choice of the machine model is governed by the application and the type of hardware to be used. The models available are the voltage model, based on the measurement of stator voltage and current, and the current model, based on the measurement of stator current and mechanical speed.

The voltage model is based on the following equations

$$\Psi_s = \int (u_s - r_s i_s)\, dt \tag{1}$$

$$\Psi_r = k_r(\Psi_s - \sigma x_s i_s). \tag{2}$$

The equations show that the accuracy of the model depends on a precise alignment of the respective values of stator resistance and leakage inductance of the model with those of the machine. For higher speeds, the stator resistance drop can be neglected, which makes the model partly insensitive in the upper speed range. However, this model is not suitable for low-speed operation. Difficulty in the accurate integration of a low-frequency quantity and the dependence on the stator resistance cause a false estimation of the rotor flux vector at low speeds. The lowest frequency of operation of this model is limited to about 3–5% of the rated frequency. The advantage of this model is that it does not require speed measurement. Hence, the model is useful in application where low-speed operation is not required or speed measurement is undesired.

The current model is usually implemented in field coordinates (see Fig. 1) and described by the following equations:

$$T_r\, di_{mr}/dt + i_{mr} = i_{sd} \tag{3}$$

$$\omega_s = \omega_m + i_{sq}/T_r i_{mr}. \tag{4}$$

The accuracy of this model depends on the proper setting of the rotor time constant T_r and the accurate measurement of the mechanical speed ω_m. Compared to the voltage model, the current model can operate throughout the frequency range. Moreover, the current model in field coordinates is easier to implement on standard microprocessor hardware. The model can be further simplified when the reference value of the stator current is used instead of its measured value. Thus, the current model has certain advantages over the voltage model and is suited for high-dynamic variable-speed variable-torque duty-cycle applications such as machine tools and robots.

III. Methods of Current Control

The current controllers determine decisively the performance of vector-controlled drives based on current-controlled VSI structures. There are many current controller strategies in use. The choice of the current controller depends on the specific application and determines the structure of the signal

Manuscript received September 11, 1990; revised March 22, 1991.

The authors are with the Electrical Machines and Drives Laboratory, University of Wuppertal, Wuppertal, Germany.

IEEE Log Number 9102175.

0278-0046/91/1000-0322$01.00

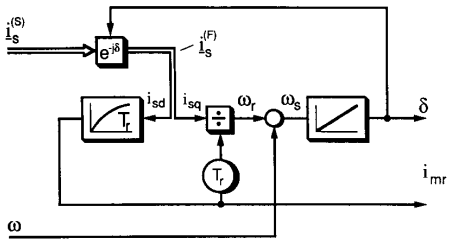

Fig. 1. Rotor model and transformation to field coordinates.

processing hardware. Possible strategies can be broadly divided into nonlinear and linear current controllers.

IV. Nonlinear Current Controllers

The simplest form of a nonlinear current controller is the hysteresis controller, It is generally implemented in stator coordinates using standard analog and digital hardware. However, these controllers have certain drawbacks such as limit cycle problems at low speeds and the variation of the current error to double the width of one hysteresis band [5]. Another form of nonlinear current controller in stator coordinates was presented in [6]. This optimizing current controller requires fast processing systems that have now become standard hardware. The method produces excellent dynamic and steady-state performance. A variation of this controller was proposed by Nabae *et al.* [7]. This method can be implemented using a conventional processor. All the above methods control the current in stator coordinates, requiring the current reference vector, inherently generated in field coordinates, to be transformed into stator coordinates. This necessitates a second vector transformation, which takes additional computing time. This can be avoided by controlling the current in field coordinates.

This problem was first addressed in [8], where current control was achieved in field coordinates. A simplified structure of a current controller in field coordinates is described by Rodriguez and Kastner [9]. Holtz and Bube [10] present an off-line optimized current control in field coordinates. The trend is toward full digital solutions of these schemes.

V. Linear Controllers

Linear controllers are generally proportional integral (PI) controllers in stator or field coordinates. PI-type current controllers, when implemented in stator coordinates, may exhibit instability problems [11]. These problems occur due to a coupling effect between the phases. Generally, PI current controllers are implemented in field coordinates [12], as shown in Fig. 2. Due to the inherent cross-coupled structure of the induction machine, decoupling terms are used to improve the dynamics of the current control loop. However, when the controller repetition time is fast enough (< 1 ms), no decoupling terms are required. Unlike nonlinear controllers, where the inverter switching state is controlled directly, the output of the linear current controller—representing the voltage reference—is applied to a PWM generator.

It is also possible to use open-loop current controllers, where the reference value of voltage is calculated from the

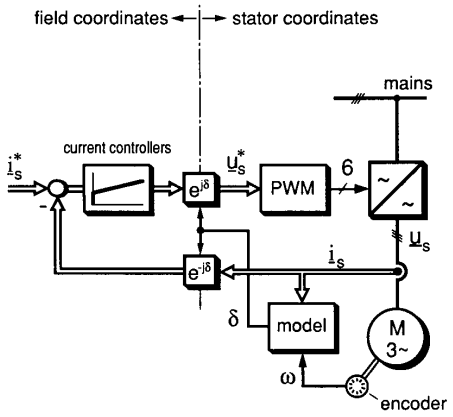

Fig. 2. Linear current control in field coordinates.

reference value of current and the machine parameters. Such a structure does not require a current measurement [13].

VI. PWM Methods

The PWM generator shown in Fig. 2 can be of different types. The standard PWM generator is of the suboscillation type. VLSI chips are commonly available for this purpose. Special reference waveforms have to be generated in order to achieve a higher modulation index [14]. The space vector modulator [15] inherently provides a high modulation index. ASIC's have become recently available that perform the PWM function. Such an ASIC can be programmed to operate at any particular switching frequency [16]. This chip also performs the transformation from field coordinates to stator coordinates. A processor-implemented space vector modulator can perform the same functions and has certain flexibility over hardware solutions. The switching time instants are stored in EPROM's. The performance can be improved by using improved space vector modulation techniques. [17], [18].

VII. Implemented Scheme

Evaluating the above options, a scheme for a high-performance vector-controlled drive has been worked out, (Fig. 3). The rotor flux identification is based on a current model in field coordinates. The current controllers are PI controllers operated in the field coordinates. The ASIC described in [16] is used here as the PWM module. The whole system is implemented on an Intel 80C196 microcontroller operating at 12 MHz clock frequency. The software is structured in a modular concept. The modules are formed depending upon their function and repetition time.

The initialization module is executed in the very beginning. In this module the machine parameters are identified and the parameters of the current, flux, and speed controllers are computed. The module initially checks the proper connection of the external hardware, such as position encoder and phase sequence. After setting all the system parameters, the processor executes the main program. The main program is an infinite loop, which services a serial interface connected to a PC or a hand-held user interface. The current module is

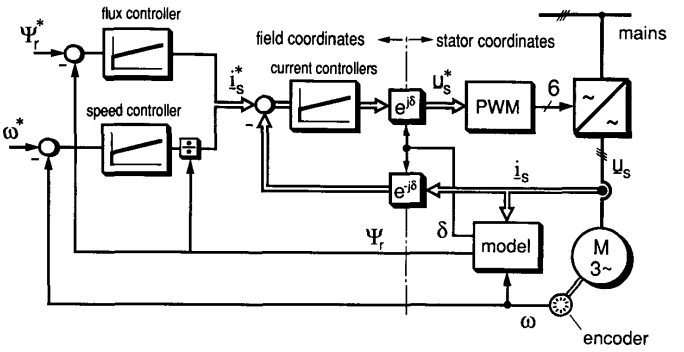

Fig. 3. Field-oriented control scheme.

organized as an interrupt service routine within this program. Each module is explained in detail in the following sections.

VIII. Initialization Module

In this module, the stator resistance and the stator transient time constant are first determined and the current controllers are then set. With the current control loops operating, the rotor time constant for the flux identification model is determined. The flux controller can be then set depending on these values. The reference value of flux or, in this case, the reference value of rotor magnetizing current, is determined next. Ultimately, the mechanical time constant is determined and the speed controller is set.

IX. Parameter Identification

A number of schemes [20]–[22] are proposed for parameter identification in the recent literature. Reference [20] describes a method for measurement of the rotor time constant, based on reactive and active power calculation. The accuracy of this method depends on how the losses are modeled. Heinemann and Leonhard [22] calculate most of the parameters using nameplate data. The actual tuning is done on line. However, the whole process of self-commissioning requires a numerical coprocessor. The method described in [21] is practical and simple to implement, but is not described in detail. This paper presents an improved algorithm that can be implemented on a microcontroller without extra hardware.

The list of the unknown parameters is

1) stator resistance r_s,
2) stator transient time constant σT_s,
3) rotor time constant T_r,
4) rotor magnetizing current i_{mrR} for rated flux, and
5) mechanical time constant T_m.

The identification process for each parameter is described as follows.

The nameplate data of the machine, indicating rated voltage, rated current, rated frequency, and number of poles, is read into the initialization module. These data are fed by the operator through a user interface before the program begins with the identification process.

The stator resistance can be determined by a test at dc level, where the applied voltage-to-current ratio is measured. The applied voltage is calculated by multiplying the modulation index of the pulse modulator with the dc link voltage. However, due to the dead time of the inverter, the actual value of the voltage is less than its calculated value. The error due to the dead time can be separated out by performing two dc tests at different modulation indexes. The PI controllers are used here to force a constant current into the machine. The parameters of these controllers are roughly set. A dc current equal to the rated machine current is forced into the machine windings by applying a single voltage space vector, the amplitude of which is PWM controlled. The same test is done for half the rated current. From these two tests the ratio of voltage to current is calculated. This method is safer than applying only the open-circuit voltage, which may lead to overcurrents in the machine and the inverter.

Next, the stator transient time constant is measured. For this test, the inverter is controlled through a binary processor port while the pulse modulator is disabled. A voltage pulse is applied to the machine by selecting an arbitrary switching state of the inverter. The duration of this pulse is initially only a few microseconds. The peak current produced by this pulse is measured. The time duration of the voltage pulse is then increased in subsequent steps until the current pulse has achieved about 30% of the rated current.

The current pulse response is shown in Fig. 4, showing that the current rises linearly. The transient time constant of the machine is now calculated in the following way. From the stator voltage equation, the flux term can be neglected as the pulse is applied to a machine that is not energized: the initial flux is zero. The rate of change of flux for this small time interval is also zero. This results in the following equation:

$$u_s = r_s i_s + \sigma l_s \, di_s / dt. \tag{5}$$

The transient time constant can be calculated from Fig. 4 as follows:

$$\sigma T_s = \frac{U \cdot T_{\text{spike}}}{r_s \cdot I_{\text{spike}}}. \tag{6}$$

The test is carried out a number of times, and the time constant is taken as the average over all these readings. The current controller parameters are set using the above results.

The current control loop is shown in Fig. 5. The open loop consists of the sample-and-hold circuit, the inverter, the

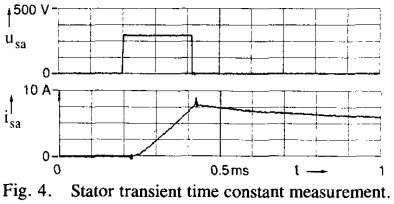

Fig. 4. Stator transient time constant measurement.

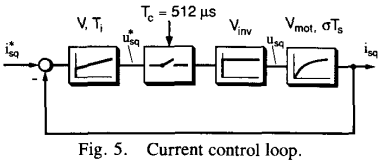

Fig. 5. Current control loop.

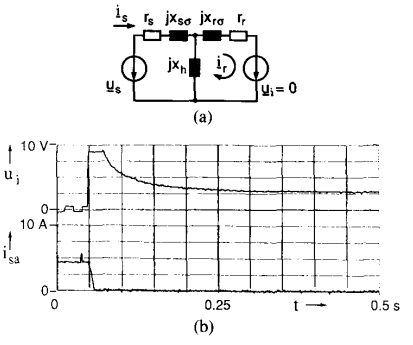

Fig. 6. Rotor time constant measurement. (a) Equivalent circuit of the machine; (b) voltage and current waveforms.

motor, and the PI controller. The controller parameters are selected based on the magnitude optimum approach [19].

$$V_{pi} = \frac{\sigma T_s}{2T_l \cdot V_{\text{mot}} \cdot V_{\text{inv}}} \tag{7a}$$

$$T_i = \sigma T_s. \tag{7b}$$

The d axis and the q axis current control loops are symmetrical; hence, the same parameters are used for both of them. The rotor time constant is determined next. A dc current is injected into the machine for some seconds, and the the rotor flux builds up as defined by

$$\Psi_r = l_h i_s. \tag{8}$$

The inverter is then turned off, open circuiting the machine. The equivalent circuit of the machine is represented by Fig. 6(a). At this time instant, the rotor flux retains its value and is solely produced by the rotor current given by

$$\Psi_r = l_r i_r. \tag{9}$$

The voltage induced in the stator can be described by the following equations:

$$u_i = \frac{l_h \, di_r}{dt} \tag{10a}$$

$$T_r \frac{di_r}{dt} + i_r. \tag{10b}$$

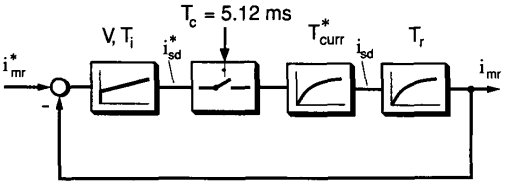

Fig. 7. Flux control loop.

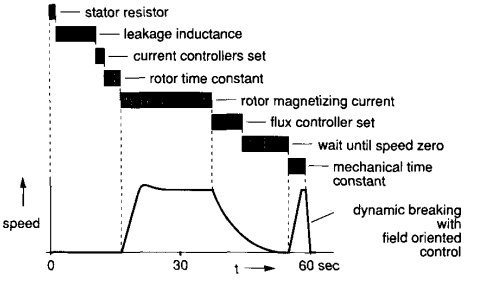

Fig. 8. Timing diagram for parameter identification.

With the machine open circuited, the voltage fades away exponentially as shown in Fig. 6(b). The rotor time constant can be obtained in good approximation using the following equation:

$$T_r = \frac{u(t)}{u(t_1) - u(t_2)} \cdot (t_1 - t_2). \tag{11}$$

The induced voltage is very small, and hence it is measured directly using an opamp without attenuation. For normal operation the opamp output voltage is limited by Zener diodes to avoid saturation.

As the rotor time constant is known, a field orientation can be carried out. As compared to [21], a simpler method is used here to determine the rated value of magnetizing current. The machine is run in open loop to half the rated frequency using the v/f ratio. The no-load current is measured and transformed into field coordinates. The rotor time constant is corrected until the q component of current is zero. The value of the d component of current is then equal to the rotor magnetizing current.

The field-weakening characteristic is calculated from the rotor magnetizing current and stored in the memory. During this test, as the motor is running, the speed is also measured. If the speed measurement is not successful, further tests are stopped and an error message is given.

Knowing the measured parameters, the flux controller is designed. The flux control loop is shown in Fig. 7. This loop consists of a lag time, the inner current loop, and a first-order delay. The parameters can be calculated using the magnitude optimum approach.

After the machine has come to a complete standstill, the test for the determination of the mechanical time constant is carried out. The machine is accelerated from standstill to a preset value of speed ω_{end} by applying a constant torque. This is performed operating the current controllers with field orientation at values i_{sq} and i_{mr}. The speed rises linearly with time. The acceleration time t_a is measured and the

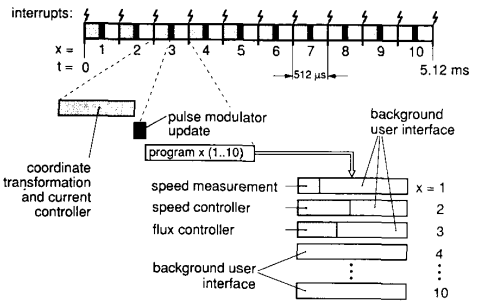

Fig. 9. Timing diagram of the field-oriented control.

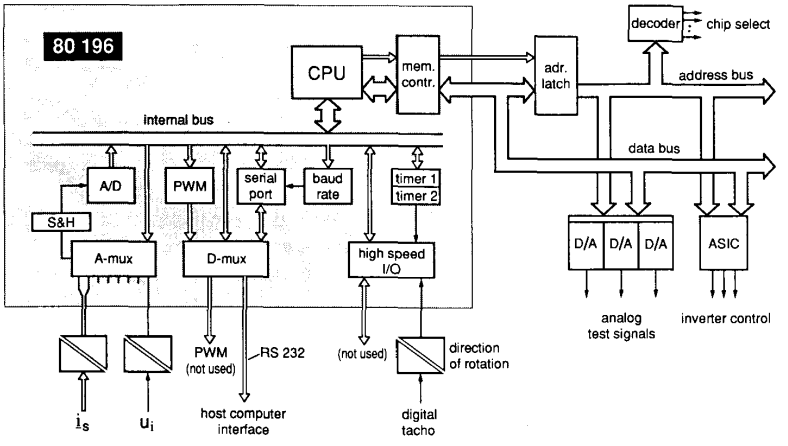

Fig. 10. Microcontroller system.

mechanical time constant is calculated using the following equation:

$$T_m = \frac{l_h^2}{l_r} \cdot \frac{i_{sq} \cdot i_{mr} \cdot t_a}{\omega_{\text{end}}}. \tag{11}$$

The speed controller is then set using the symmetrical optimum approach. Fig. 8 shows the timing diagram for the identification process. The total time t_{ini} for the parameter identification scheme is 60 s.

With the identification completed, the program initializes all the controller outputs and the pulse modulator and exits this module. The acquired parameters are stored in an EEPROM and a flag is set to indicate that the commissioning is already done. Subsequent starts of the drive will not execute the identification process. Another option allows the user to totally circumvent the self-commissioning process. Fine-tuning of the parameters is possible through the serial data link.

X. Field-Oriented Control Software

This module is an interrupt service routine for the pulse modulator interrupt. It is repeated every 512 µs. The current is sampled on an interrupt from the PWM module to force the synchronization between the modulator and the current sampling instant. The incremental encoder output is also sampled at the same instant. The sampled current is transformed into field coordinates. Then the two current controllers are executed to calculate the vector components of the reference voltage. The rotor flux position is calculated next. These values along with the value of preset switching frequency are transferred to the PWM module. This forms the first part of the interrupt service routine.

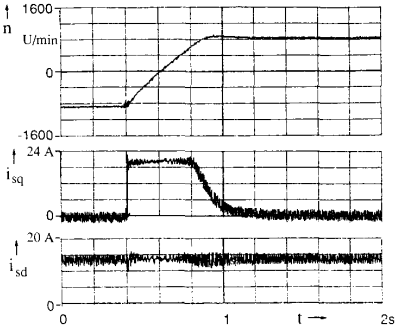

Fig. 11. Speed reversal at 800 r/min.

In the second part of the interrupt service routine the speed controller, the flux controller, and the calculation of rotor flux magnitude are executed every 5.12 ms, i.e., every tenth current loop. The timing diagram for this module is shown in Fig. 9. Fig. 10 shows the hardware architecture of the microcontroller system.

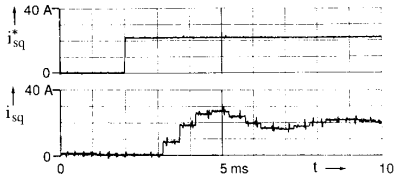

Fig. 12. Dynamic response of the current controller.

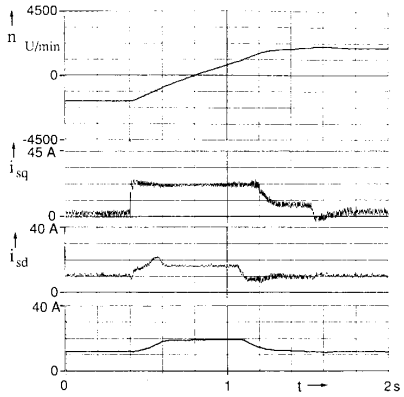

Fig. 13. Speed reversal at 2200 r/min.

XI. Experimental Results

The experimental results are obtained from a 25-kVA inverter fed induction motor drive. Fig. 11 shows the speed reversal at 800 r/min. The response of the current control loop is shown in Fig. 12. Fig. 13 shows the speed reversal at 2200 r/min with field weakening.

XII. Conclusion

A field-oriented control using the rotor model in field coordinates is realized using standard microcontroller hardware. An ASIC for pulse-width modulation makes the system compact. The self-commissioning scheme is implemented with low computing overhead and does not require an extra numeric processor. The on-chip serial data link permits master–slave operation and serves for monitoring and diagnostic purposes.

References

[1] F. Blaschke, "Das Prinzip der Feldorientierung, die Grundlage für die Transvector-Regelung von Asynchronmaschinen," *Siemens-Zeitschrift*, vol. 45, pp. 757–760, 1971.

[2] K. Hasse, "Zur Dynamik drehzahlgeregelter Antriebe mit stromrichtergespeisten Aysnchronkurzschlußläufer maschinen," Ph.D. dissertation, TH Darmstadt, 1969.

[3] R. Gabriel and W. Leonhard, "Microprocessor control of induction motor," in *Proc. Int. Semiconductor Power Converter Conf.*, Orlando, FL, 1982, pp. 385–396.

[4] R. Jötten and G. Maeder, "Control methods for good dynamic performance induction motor drives based on current and voltage as measured quantities," in *Proc. IEEE/IAS Int. Semiconductor Power Converter Conf.*, Orlando, FL, 1982, pp. 397–407.

[5] D. M. Brod and D. W. Novotny, "Current control of VSI-PWM inverters," in *Proc. IEEE Ind. Appl. Soc. Ann. Mtg.*, Chicago, IL, 1984, pp. 418–425.

[6] J. Holtz and S. Stadtfeld, "A predictive controller for the stator current vector of ac machines fed from a switched voltage source," in *Proc. Int. Power Electron. Conf. IPEC*, Tokyo, Japan, 1982, pp. 692–697.

[7] A. Nabae, S. Ogasawara, and H. Agaki, "A novel current control scheme for current-controlled PWM inverters," in *Proc. IEEE/IAS Ann. Mtg.*, Toronto, 1985, pp. 473–478.

[8] J. Holtz and S. Stadtfeld, "Field-oriented control by forced motor currents in a voltage fed inverter drive," in *Proc. IFAC Symp. Control Power Electron. Electrical Drives*, Lausanne, Switzerland, 1983, pp. 103–110.

[9] J. Rodriguez and G. Kastner, "Nonlinear current control of an inverter-fed induction motor," *ETZ-Archiv*, pp. 245–250, 1987.

[10] J. Holtz and E. Bube, "Field-oriented asynchronous pulsewidth modulation for high performance ac machine drives operating at low switching frequency," in *Proc. IEEE/IAS Ann. Mtg.*, Pittsburgh, PA, 1988, pp. 412–417.

[11] D. Seifert, "Stromregelung der Asynchronmaschine," *ETZ-Archiv*, pp. 252–256, 1986.

[12] W. Schumacher and G. Heinemann, "Fully digital control of induction motor," in *Proc. 1st European Power Electron. Conf.*, Brussels, Belgium, 1987, pp. 2.191–2.196.

[13] R. Joensson, "Measurements of a new ac induction motor control system," in *Proc. European Power Electron. Conf.*, Aachen, Germany, 1989, pp. 17–22.

[14] D. A. Grant and J. A. Houldsworth, "PWM ac motor drive employing ultrasonic carrier," in *Proc. IEE Power Electron. Variable-Speed Drives Conf.*, London, 1982, pp. 237–240.

[15] J. Holtz, P. Lammert, and W. Lotzkat, "High-speed drive system with ultrasonic MOSFET-PWM-inverter and single-chip-microprocessor control," in *Proc IEEE/IAS Ann. Mtg.*, Denver, CO, 1986, pp. 12–17.

[16] E. Kiel, W. Schumacher, and R. Gabriel, "PWM gate array for ac drives," in *Proc. 2nd European Power Electron. Conf.*, Grenoble, France, 1987, pp. 653–658.

[17] S. Ogasawara, H. Agaki, and A. Nabae, "A novel PWM scheme of voltage source inverters based on space vector theory," in *Proc. European Power Electron. Conf.*, Aachen, Germany, 1989, pp. 1197–1202.

[18] J. Holtz and L. Springob, "Reduced harmonics PWM controlled line-side converter for electric drives," presented at the *IEEE/IAS Ann. Conf.*, Seattle, WA, 1990.

[19] F. Fröhr and F. Orttenburger, *An Introduction to Electronic Control Engineering*. Berlin: Siemens AG, 1982.

[20] T. Irisa, S. Takata, R. Veda, T. Sonoda, and T. Mochizaki, "A novel approach on parameter self-tuning method in ac-servosystem," in *Proc. IFAC Symp. Control in Power Electron. Electrical Drives*, (Lausanne, Switzerland, 1983), pp. 41–48.

[21] H. Schierling, "Fast and reliable commissioning of ac variable speed drives by self-commissioning," in *Proc. IEEE Ind. Appl. Soc. Ann. Mtg.*, Pittsburgh, PA, 1988, pp. 489–492.

[22] G. Heinemann and W. Leonhard, "Self-tuning field oriented control of an induction motor drive," in *Proc. IPEC Int. Power Electron. Conf.*, Tokyo, 1990, pp. 465–472.